

FEM simulation of the viscous effects of loading rate on Albany sand

ABU HENA MUNTAKIM¹, MOHAMMED SAIFUL ALAM SIDDIQUEE²

¹Department of Civil Engineering, Bangladesh University of Engineering and Technology, Bangladesh

²Department of Civil Engineering, King Abdul Aziz University, Jeddah, Kingdom of Saudi Arabia

Email: muntakim786@gmail.com,msa.sid@gmail.com

Abstract: In this research, effect of strain rate on the albany sand has been studied by elastic visco-plastic constitutive model within the three component framework. Strain rate effect can be modeled by using any one of the (i) isotach, (ii) tesra (temporary effects of strain rate and acceleration) or viscous evanescent and (iii) p & n (positive and negative viscosity), models of the three component framework. Usually “isotach” is appropriate for clay and soft rock, “tesra” is appropriate for sand and “p & n” is appropriate for sand with less angularity like albany sand. Here in this research triaxial compression (tc) tests results of albany sand at different strain rate has been modeled successfully into a commercially available package called “abaqus”. The p&n model was implemented into a generalized elasto-plastic isotropic strain-hardening non-linear model in C++. The model is then embedded in the finite element computer program abaqus. Abaqus was used for the actual analysis. In order to define p & n model, user subroutine of abaqus “umat” was written in C++ and used. Abaqus is such a robust fem software that allows writing subroutines for describing material behavior. Generally umat is written in fortran but in this study, the main model is written in C++ and then it is called by fortran with appropriate change in abaqus environment file. Without spending any significant extra computational time or storage this p & n model embedded in fe code can simulate the time-dependent stress-strain behavior accurately.

Keywords: Constitutive Law, Numerical Simulation, Three Component Framework, P&N Model, Elasto-Plastic Model, UMAT

1. Introduction:

In recent decades, problems related with long-term creep deformation of sand deposit loaded with a heavy superstructure or secondary consolidation of saturated soft clay including a number of full-scale field cases have attracted the attention of Geotechnical engineers for correctly understanding and accurately evaluating the viscous properties of geomaterials. Highly non-linear relationships of soil were the main obstacles in soil mechanics. With the development of different experimental and analytical methods, various constitutive models for defining soil behavior have been published.

For simulating the effects of material viscosity on the stress-strain behavior of geomaterial (i.e., clay, sand, gravel, and sedimentary softrock), a set of stress-strain models within the framework of the general non-linear three-component model (Di Benedetto et al., 2002 and Tatsuoka et al. 2002) have been proposed by researchers. Three basic viscosity types have been published which are (i) Isotach, (ii) TESRA (Temporary Effects of Strain Rate and Acceleration) or Viscous Evanescent, (iii) P & N (Positive and Negative viscosity).

P & N viscosity type has been used to simulate the stress-strain behaviour of Albany sand, fine silica sand from Australia. This type of viscosity is very peculiar and was found most recently.

2. Experimental results:

From the laboratory experiments (Tatsuoka et al.2008), it was found that four poorly graded granular materials named a) corundum A

(Aluminium Oxide, Al_2O_3), an artificial material ($e_{max} = 1.066$ & $e_{min} = 0.865$); b) Albany sand, a fine silica sand from Australia ($e_{max} = 0.804$ & $e_{min} = 0.505$); c) Hime gravel, a natural fine gravel from a river bed in the Yamanashi Prefecture, Japan ($e_{max} = 0.759$ & $e_{min} = 0.515$); and d) Monterey No. 0 sand, a natural fine beach sand from the USA ($e_{max} = 0.860$ & $e_{min} = 0.550$), exhibited the P & N viscosity in the drained TC tests. In this paper, the experimental results of Albany sand are the main focus.

Loose and dense cylindrical specimens of diameter of 70 mm and height of 150-155 mm were prepared from Albany sand. The experiments were performed on air-dried specimens to keep the loading rate effects out of the effects of delayed dissipation of excess pore water pressure.

A 0.3 mm thick latex rubber disc smeared with a 0.05 mm thick silicon grease layer (Tatsuoka et al., 1984) was used at the top and bottom ends of the each specimen. An external deformation transducer and a pair of local deformation transducers (L D T s; Goto et al., 1991) which had a gauge length of about 12cm, was used to measure axial deformation. The homogeneity in the zone of before and after peak, was not possible to evaluate. The reason of this phenomenon was discussed by Tatsuoka et al. (1990) and it was showed that local shear bands start developing before the peak stress state in drained plane strain compression (PSC) tests on dense sand. Locally measured axial strains were used to calculate the elastic deformation properties. Based on the modified Rowe's stress-dilatancy relation, the

volume change of air dried specimen was estimated. These experiments were done using an automated triaxial apparatus (e.g., Santucci de Magistris et al., 1999).

The specimens were loaded automatically. To control the cell pressure, a high precision gear-type axial loading system driven by a servo-motor together with an electric pneumatic pressure transducer was used. By increasing the effective stress from 20 kPa toward 400 kPa, at an axial strain rate of 0.0625%/min, the isotropic compression was performed. During the isotropic compression process, to evaluate the vertical quasi-elastic Young's modulus, eight cycles of an axial strain (double amplitude) of 0.001-0.003% were applied at $p^*=50, 100, 200$ and 300 kPa.

Figure 1 illustrates results from three sets of drained TC tests performed at largely different constant axial strain rates on dense air dried specimens of Albany sand.

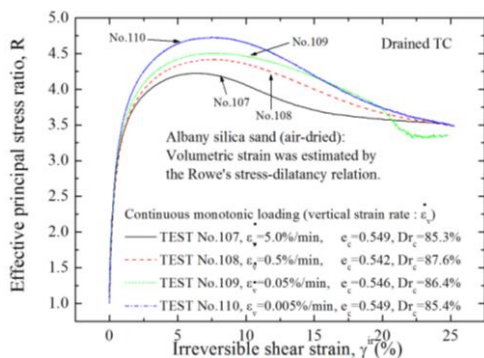


Figure 1: Results from CD TC tests at different vertical strain rates on air dried dense Albany silica sand

3. Methodology:

The modelling of stress-strain behavior of geomaterial is very challenging as stress-strain behavior is highly non-linear. Development of FEA finds a way to solve the boundary value problem with highly non-linear material property. There are many commercially available FEM software now-a-days. Among them Abaqus is a robust software that allows user to model their own material model using user subroutine. But the challenge arises when user wants to write their material model in other language rather than FORTRAN. In this study, this challenge has been successfully handled as the user subroutine for material model has been written in C++ and used.

3.1 Pseudo-Algorithm:

Siddiquee et al. (2006) had developed the pseudo-algorithm which was the revised form of original solution technique of the DR method. Viscous effects were not included.

In "return mapping algorithm" (Ortiz and Simo, 1986), incremental elasto-plastic equations are solved at the first level of integration. Satisfying the consistency condition (abiding by the flow rule), the stress is returned to the growing yield surface. When calculating the viscous stress based on P&N model,

the stress is returned to the inviscid yield surface with an incremental integration during the second level of integration when it is necessary at each step of return mapping iteration. This scheme is presented in Fig 2.

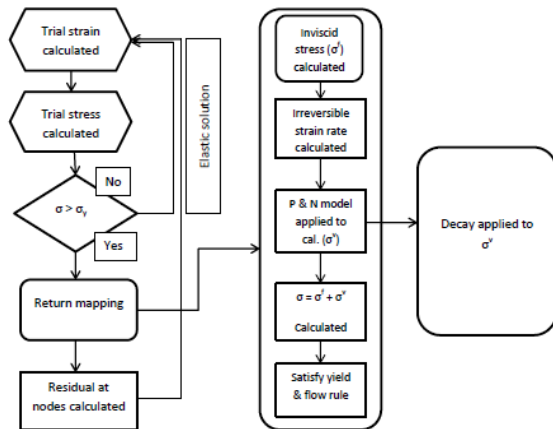


Figure 2: Implementation of the "P & N" model into a FEM code

3.2 Over-all model calculation functions:

In the user subroutine "UMAT", the stress and hardening softening parameters are calculated from strain and elastic modulus provided by Abaqus. With the updated stress and hardening softening parameters Abaqus carry out the non-linear boundary solution and provide strain and elastic modulus to "UMAT". In this process, the whole analysis is completed. The main function of user subroutine "UMAT" is UMAT_CPP. In UMAT_CPP the strain calculated by Abaqus solver is taken as input and it calculates the stress in that given moment. At the end of this function, the stress is updated to Abaqus. In this function the elastic modulus is calculated from Young's modulus and Poisson ratio. Failure surface is calculated in the function ReturnMapping_. PlasticModel_ function calculates the reference curve. The function yldchk_ calculates the yield function. The calculation of Invariants is done in the function invar_. The potential function and yield function is calculated in the function yieldf_.

3.3 Material Model Description:

Di Benedetto et al., 2002; Tatsuoka et al., 2002. successfully simulated the rate dependent stress-strain behaviour of geomaterial observed in a number of laboratory stress-strain tests by the non-linear three-component model (Fig. 3).

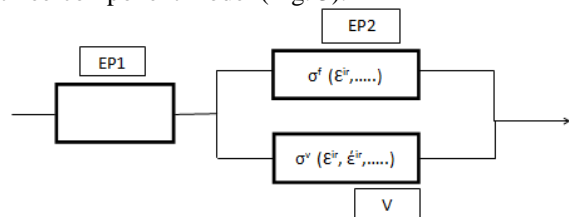


Figure 3: Non-linear three-component model (Di Benedetto and Tatsuoka, 1997; Di Benedetto et al., 2002; Tatsuoka et al., 2002)

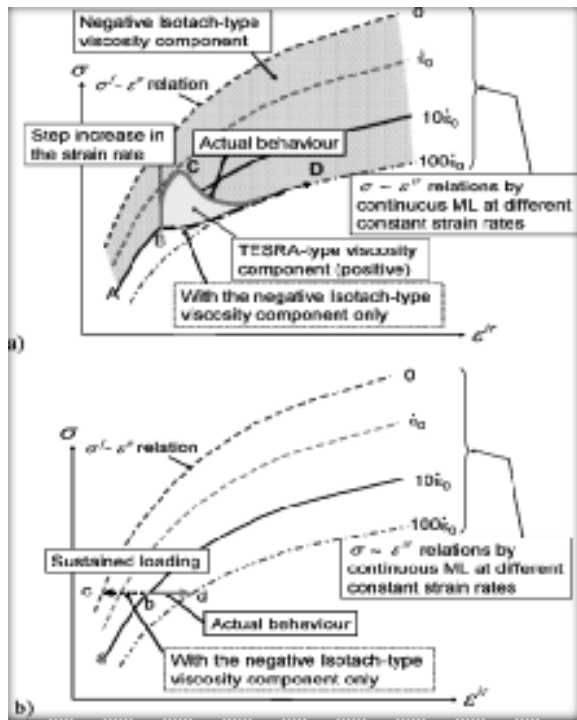


Figure 4: Illustration of P & N viscosity

Figure 4 illustrate the P&N viscosity type (Tatsuoka et al. 2008), which is defined below:

In this type of viscosity, the viscous stress increment that developed at a given moment during subsequent loading decays with an increase in instantaneous irreversible strain towards different residual values. The strength during ML at a constant ϵ decreases with an increase in ϵ .

In the framework of the three-component model the measured stress, σ , consists with two parts which are the inviscid stress component, σ^f , and the viscous stress component, σ^v at the same ϵ^{ir} . Negative isotech type is a feature of σ^v . Both positive TESRA type component and negative Isotech type component at other strain rate are the components of σ^v . This can be observed when a step increase in $\dot{\epsilon}$ at point B during otherwise ML at a constant. The stress strain behavior should be like A→B→D if there are only negative Isotech type component. But the behavior like A→B→C→D, instead of A→B→D is observed

in poorly graded relatively round and stiff-particle granular material. A step increase in $\dot{\epsilon}$ (B→C) results same amount of immediate positive stress increase when the viscosity type is Isotech or Combined or TESRA (Temporary Effects of strain Rate and Acceleration). After that subsequent ML at a constant $\dot{\epsilon}$ results decrease of σ^v from a temporarily increased value (C→D) like the TESRA type. This feature was also found in the stress-strain behavior of Albany sand. For this reason P & N model is the appropriate viscosity type for simulating viscosity of Albany sand.

3.4 Computational Setup:

Abaqus/CAE, or "Complete Abaqus Environment" (a recursive acronym and backronym with an obvious root in Computer-Aided Engineering) is used for both for the modelling and analysis of mechanical components and assemblies (pre-processing) and visualizing the finite element analysis result.

Full computational setup scheme described below.

G1: Installation of the finite element software ABAQUS, FORTRAN compiler and C++ compiler.

G2: Change in windows environment variable to make FORTRAN and C++ compiler available to CMD.

G3: Change in ABAQUS environment file to make .lib and .dll file available for ABAQUS.

G4: Run the verification exe to check all components are compatible with each other.

The material model code was written in C++ then it was compiled to .dll using C++ compiler. From .dll, using CMD and C++ compiler the .lib file was created. The finite element model was created using Abaqus/CAE and using FORTRAN the material model was called and performed the analysis.

4. Details of the model:

4.1 Parameters used:

Kongkitkul et al. (2008) described various aspects of the simulation. Tatsuoka et al. (2008) represented simulation parameters for the stress-strain behaviour exhibiting the P & N viscosity.

Table 1: Viscosity parameters used to analyse the CD triaxial tests

Material	Strain parameter	β : test results	Parameters in the viscosity function			Back-calculated by fitting		Decay parameter	Viscosity type parameter, Θ			
			α	m	ϵ_r^{ir}	b	β : from b		Θ_{in}	Θ_{end}	c	ϵ_{Θ}^{ir} %
Albany sand	Irreversible Shear strain	0.0195	0.24	0.04	1.0E-5(%/s)	0.00827	0.0190	1.0E-03	-0.3	-1.0	1.0	12

4.2 Elasto-plastic framework:

The present study is done using the generalized elasto-plastic isotropic strain-hardening and softening model which takes into account strain localization associated with shear banding by introducing a characteristic width of shear band in the additive elasto-plastic decomposition of strain (Tatsuoka et al., 1993). The yield function is used as follows:

$$\Phi = -\eta I_1 + \frac{1}{g(\Theta)} \sqrt{J_2} - K \quad (1)$$

The above equation is used as the growth function of the yield surface of the generalized Mohr-Coulomb type. Where I_1 is the first stress invariant (i.e., hydrostatic stress component, positive in compression); and J_2 is the second deviatoric stress invariant (i.e., the deviatoric stress). Siddiquee et al. (1999, 2001a and b) had explained in detail about the growth function.

The plastic potential function, ψ , is defined as;

$$\Psi = -\alpha I_1 + \sqrt{J_2} - K \quad (2)$$

This plastic potential function, of the Drucker-Prager type, is similar to the yield function except that $g(\Theta)$ in equation 1. Here in the analysis, stress dependent elastic parameters are used.

5. Results and discussions:

Four different strain-rate experimental results are simulated successfully in this study.

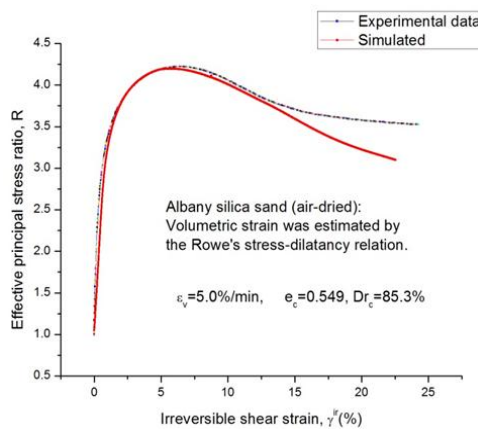


Figure 5: Experimental and simulated curve of Effective principal stress, R vs Irreversible shear strain at a vertical strain rate 5.0%/min

In Fig. 5, the simulated curve has been compared with the experimental data of TC test at a vertical strain rate 5.0% / min. In this simulation, the peak effective principal stress was 4.22 at irreversible shear strain 6.6%. The simulated curve is largely deviated from experimental curve after irreversible shear strain 13.4%.

In Fig. 6, the simulated curve has been compared with the experimental data of TC test at a vertical strain rate 0.5%/min. In this simulation, the peak effective principal stress was 4.4 at irreversible shear strain 8.2%. The simulated curve is largely deviated from experimental curve after irreversible shear strain 5.51%.

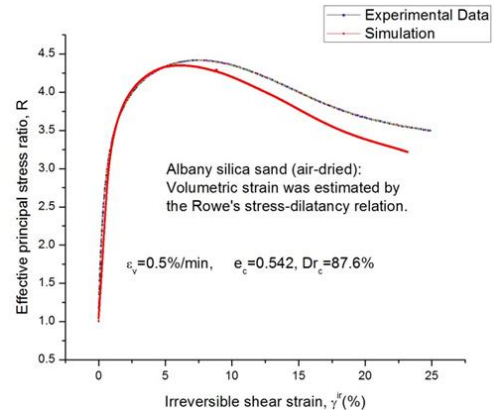


Figure 6: Experimental and simulated curve of Effective principal stress, R vs Irreversible shear strain at a vertical strain rate 0.5%/min

In Fig. 7, the simulated curve has been compared with the experimental data of TC test at a vertical strain rate 0.05%/min. In this simulation the peak effective principal stress was 4.5 at irreversible shear strain 7.5%. The simulated curve is largely deviated from experimental curve after irreversible shear strain 9.4%.

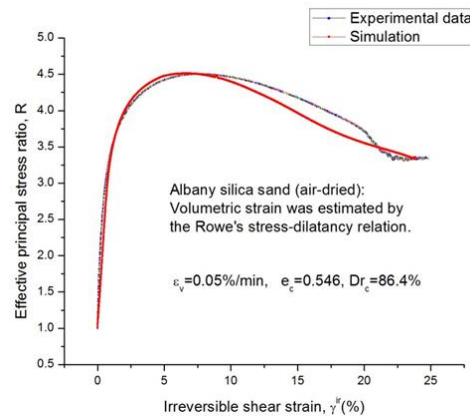


Figure 7: Experimental and simulated curve of Effective principal stress, R vs Irreversible shear strain at a vertical strain rate 0.05%/min

In Fig. 8, the simulated curve has been compared with the experimental data of TC test at a vertical strain rate 0.005%/min. In this simulation, the peak effective principal stress was 4.7 at irreversible shear strain 7.15%. As this curve is accounted as base, the simulated and experimental curve is nearly same.

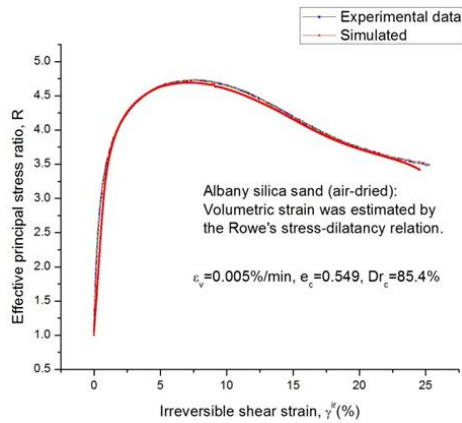


Figure 8: Experimental and simulated curve of Effective principal stress, R vs Irreversible shear strain at a vertical strain rate $0.005\%/min$

6. Conclusions:

The elastic visco-plastic analysis of the TC tests is not a new topic. However, this study was devoted to model the experimentally observed findings in a very realistic and simplified way. The yield function was Mohr-Coulomb type and plastic potential was Drucker-Prager type. The following conclusions can be drawn from this study.

1. Effect of strain rate on the Albany sand has been studied by combination of elastic visco-plastic constitutive law and three component framework.
2. TC tests results of Albany sand at different strain rate has been modelled successfully into a commercially available package called "ABAQUS".
3. The P&N model was implemented into a generalized elasto-plastic isotropic strain-hardening non-linear model in C++. The model is then embedded in the finite element computer program ABAQUS.
4. For small strain the experimental data was successfully simulated but problem was associated with large deformation. The simulated curve deviated more or less from 7.5 % irreversible shear strain. The deviation was higher for vertical strain rate at $0.3\%/min$.
5. A FORTRAN compiler is required to compile and link user subroutines for Abaqus. But it also allows writing user subroutines in languages other than FORTRAN with the FORTRAN compiler specified and a compiler for that language. It is needed to call routines in that language from FORTRAN.
6. In this study, user subroutine was written in C++ rather than FORTRAN. With the help of C++ compiler .dll and .lib file was created and they were placed in appropriated destination and the environmental file was updated. This made possible to call the user subroutine from FORTRAN and simulation of stress-strain behaviour of Albany sand.

7. Without spending any significant extra computational time or storage this P & N model embedded in FE code can simulate the time-dependent stress-strain behaviour accurately.

Acknowledgements:

The contribution of geotechnical engineering lab of University of Tokyo, Japan is deeply appreciated.

References:

- [1] Siddiquee, M.S.A., Tatsuoka, T., and Tanaka, T. (2006). "Fem simulation of the viscous effects on the stress-strain behaviour of sand in plane strain compression" *Soils and Foundations*, Vol. 46(1), 99-108.
- [2] Tatsuoka, T. Di Benedetto, H., Enomoto, T., Kawabe, S. and Kongkitkul, W. (2008). "Various viscosity types of geomaterials in shear and their mathematical expression" *Soils and Foundations*, Vol. 48(1), 41-60.
- [3] Di Benedetto, H., Tatsuoka, F. and Ishihara, M. (2002). "Time-dependant shear deformation characteristics of sand and their constitutive modelling" *Soils and Foundations*, 42(2), 1-22.
- [4] Di Benedetto, H., Tatsuoka, F. (1997). "Small strain behaviour of geomaterials: modelling of strain effects" *Soils and Foundations*, Vol. 37(2), 127-138.
- [5] Santucci de Magistris, F., Koseki, J., Amaya, M., Hamaya, S., Sato, T. and Tatsuoka, F. (1999). "A triaxial testing system to evaluate stress-strain behaviour of soils for wide range of strain and strain rate" *Geotechnical Testing Journal*, ASTM, Vol 22(1), 44-60.
- [6] Tatsuoka, F., Molenkamp, F., Torii, T. and Hino, t. (1984). "Behaviour of lubrication layers of platens in element tests" *Soils and Foundations*, Vol 24(1), 113-128
- [7] Goto, S., Tatsuoka, F., Shibuya, S., Kim, Y.-S. and Sato, T. (1991). "A simple gauge for local small strain measurements in the laboratory" *Soils and Foundations*, Vol 31(1), 169-180.
- [8] Tatsuoka, F., Nakamura, S., Huang, C.-C. and Tani, K. (1990). "Strength anisotropy and shear band direction in plane strain tests on sand". *Soils and Foundations*, Vol 30(1), 35-54.
- [9] Ortiz, M. and Simo, J. C. (1986). "An analysis of a new class of integration algorithms for elasto-plastic constitutive relations" *Int. J. Num. Meth. Engg.*, vol 23, 353-366.
- [10] Tatsuoka, F., Di Benedetto, H., Kongkitkul, W. Kongsukprasert, L. and Nishi, T. (2008). "Modelling of ageing effects on the elastoviscoplastic behaviour of geomaterial" *Soils and Foundations*, 48(2) 155-174.
- [11] Tatsuoka, F., Siddiquee, M.S.A., park, C.-S., Sakamoto, M. and Abe, F. (1993). "Modelling stress-strain relations of sand" *Soils and Foundations*, Vol 33(2), 60-81.

- [12] Siddiquee, M. S. A., Tatsuoka, F., Tanaka, T., Tani, K., yoshida, K. and Morimoto, T. (2001) “ Model tests and FEM simulation of some factors affecting the bearing capacity of footing on sand” *Soils and Foundations*, Vol 41(2), 53-76.
- [13] Siddiquee, M. S. A., Tatsuoka, F. (2001) “Modelling time dependant stress-strain behaviour of stiff geomaterials and its applications” *Proc. 10th Int. Conf. Comput. Math. Adv. Geomech.(IACMAG)*, January 7-12, Tucson, Arizona.
- [14] Siddiquee, M. S. A., Tatsuoka, F., Tanaka, T., Tani, K. and Morimoto, T. (1999) “ FEM simulation of scale effect in bearing capacity of strip footing on sand” *Soils and Foundations*, Vol 34(4), 91-109.